Oral presentation | Fluid-structure interaction
Fluid-structure interaction-I
Mon. Jul 15, 2024 10:45 AM - 12:45 PM Room A

[1-A-04] Numerical investigation of correlation between thrust and angle of attack in a cyclorotor system

*Manabu Saito[1], Jun Nagao[1], Ryoichi Kurose[1] (1. Kyoto University)

Keywords: Cyclorotor, Large-eddy simulation, Propulsion system

Numerical investigation of correlation between thrust and angle of attack in a cyclorotor system

Manabu Saito, Jun Nagao, Ryoichi Kurose

Thermal Science and Engineering Laboratory
Dept. of Mechanical Engineering and Science
Kyoto University

1

Background

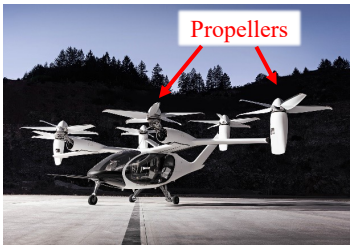

S4 ©Joby Aviation

VX4 ©Vertical Aerospace

For Urban Air Mobility (UAM) , Vertical Take-Off and Landing (VTOL) aircraft is considered.

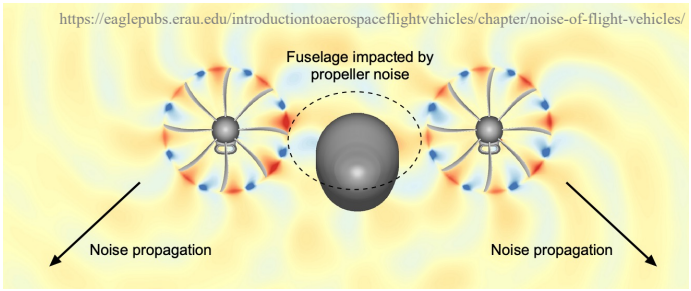

Propellers are used as a propulsion system
→ Intense noise generation has been the biggest problem

To overcome the noise problem in UAM, "**Cyclorotor**" is gaining attention as an alternative propulsion system

2

Cyclorotor

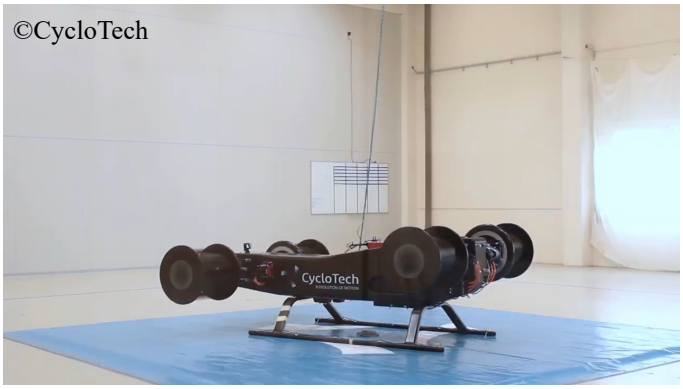

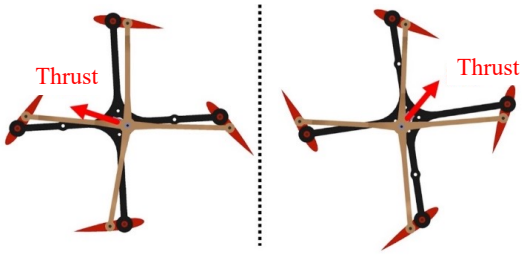

360° thrust vectoring

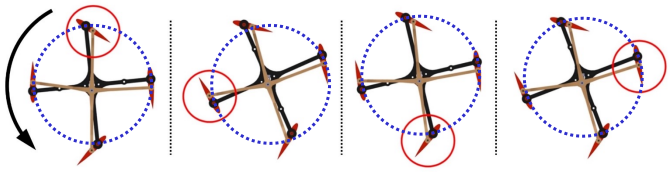

Main features of a **Cyclorotor**:
- Maneuverability - Thrust in any direction/magnitude
- Lower noise level - Lower blade-tip speed

3

Flight capability of cyclorotor-powered aircraft

Propeller

Cyclorotor

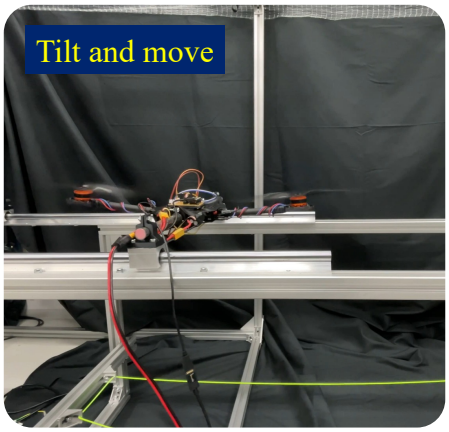

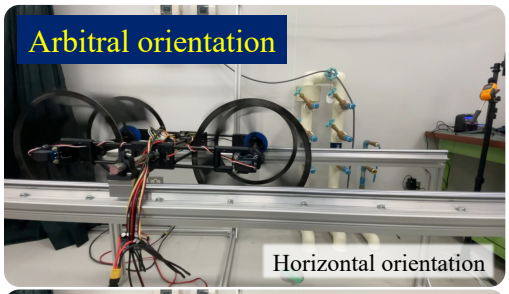

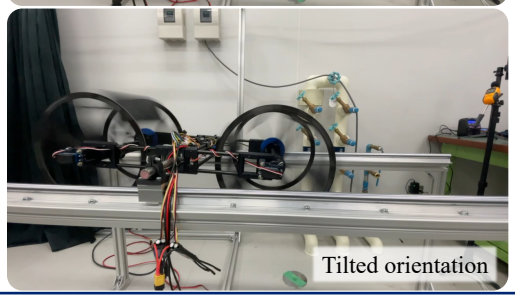

4

Flight stability against sidewind

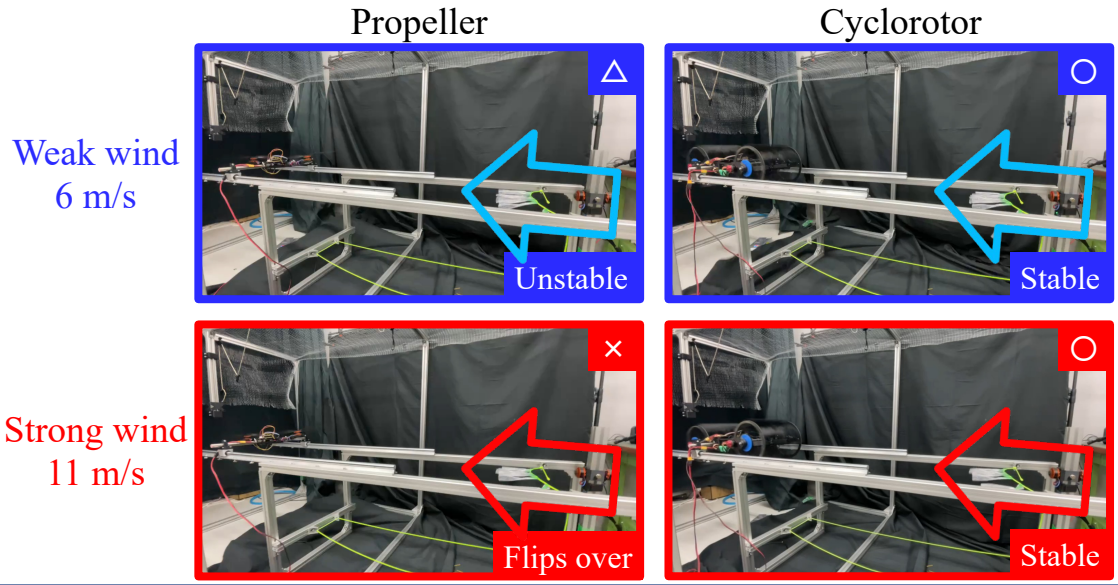

ICCFD12

5

Geometrical optimization of a cyclorotor

Optimization properties:

- Number of blades
- Airfoil shape (cross section/taper angle)
- Rotational radius
- Span length
- Angle of attack schedule

…

ICCFD12

6

Geometrical optimization of a cyclorotor

Optimization properties:

- Number of blades

To conduct an in-depth study of the aerodynamic characteristics of the airflow produced by cyclorotors using large-eddy simulations and find an optimal AoA schedule to maximize the aerodynamic performance of a cyclorotor.

- Span length
- Angle of attack schedule

…

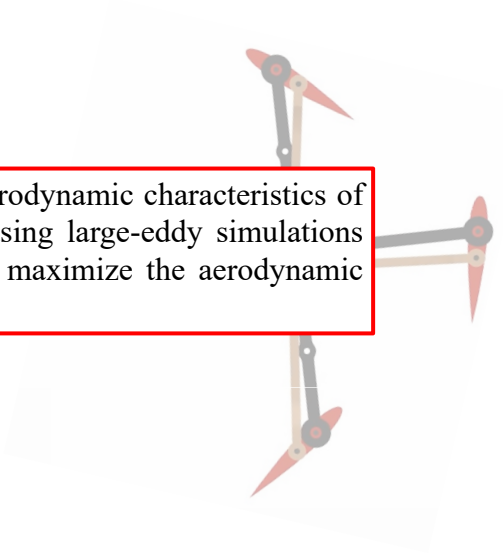

7

Computational domain

NACA0010

Cyclorotor[4]

Shape
NACA0010
Span length
150 mm
Chord length
25.4 mm
Radius (R)
60 mm
Rotational speed (Ω)
800 rpm
Reynolds number
10,000
Angle of attack
-20° ~ 20°

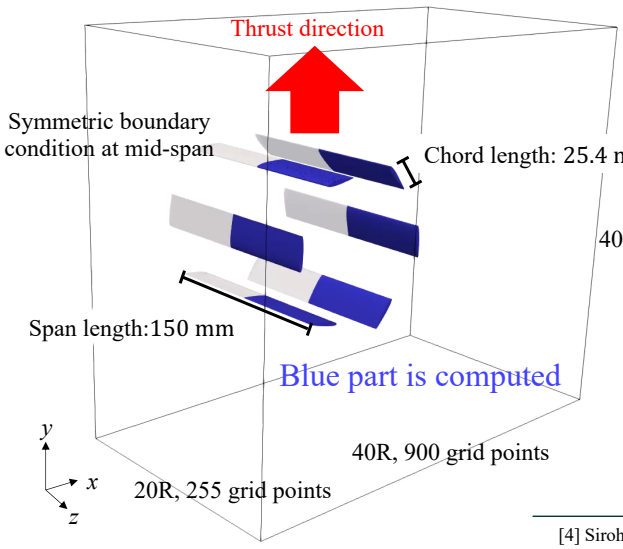

Initial condition
Static air
Pressure: 1 atm
Temperature: 300 K

Boundary condition
z-direction (-): Symmetric
Others : Outflow

[4] Sirohi et al., *J. Am. Helicopter Soc.*, 2007

8

Computational method

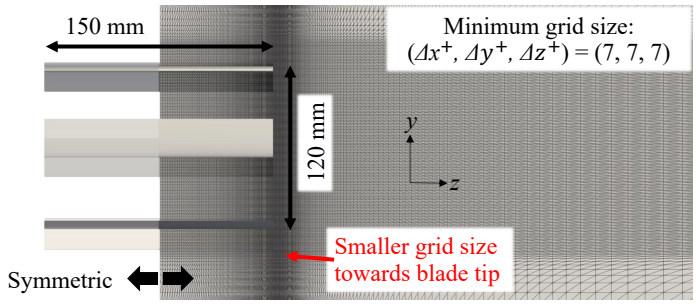

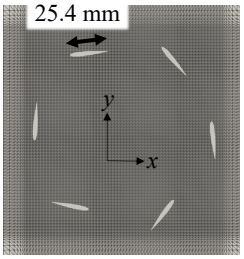

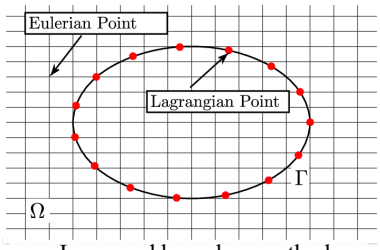

Immersed boundary method

- Incompressible N-S equations, Finite difference method (FVM)
- Number of grid points: $(nx, ny, nz) = (900,940,255)$ (total of 0.2 billion)
- Wall surface: Diffuse-interface immersed boundary method (IBM)
  (Boundary-condition enforced IBM) [5]
- Number of Lagrangian points for each blade: 28,141

[5] Pinelli et al., *J. Comput. Phys.*, 2010

9

Angle of attack schedule

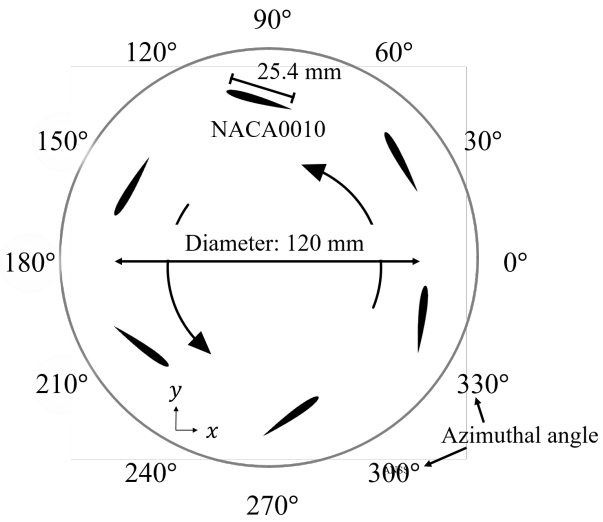

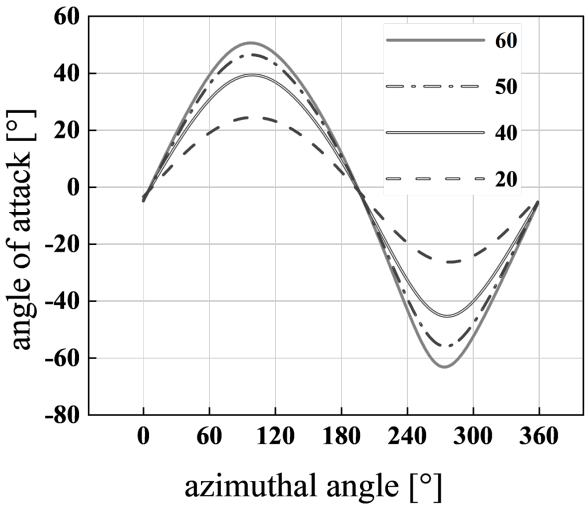

10

3D Visualization of Flow around the Cyclorotor (AoA amplitude: 20°)

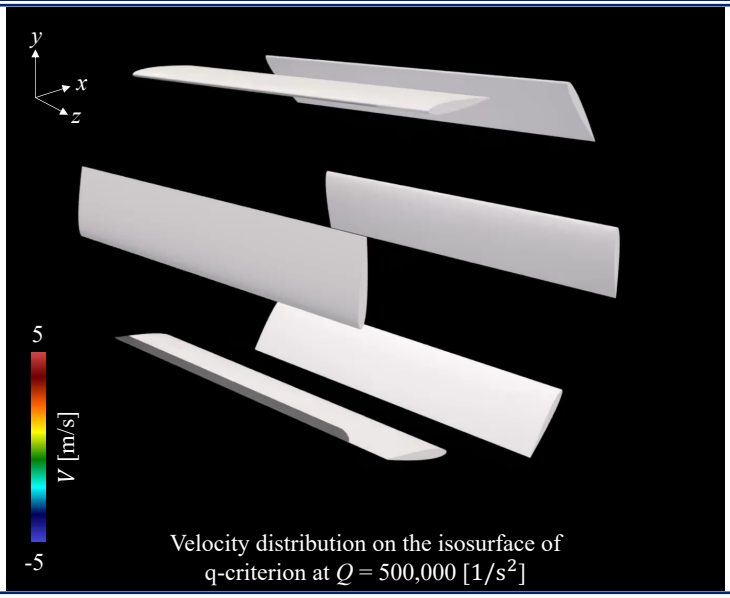

Velocity distribution on the isosurface of q-criterion at $Q = 500{,}000\ [1/s^2]$

[-]	LES	Experiment [4]
C_T	0.04661	0.04573
C_P	0.02681	0.02941

$$C_T = \frac{\text{Thrust}}{\rho \pi b_r d (\Omega R)^2}$$

$$C_P = \frac{\text{Power}}{\rho \pi b_r d (\Omega R)^3}$$

ρ : density
b_r : span length
d : Diameter
R : Radius
Ω : Rotational speed

[4] Sirohi et al., *J. Am. Helicopter Soc.*, 2007

11

Thrust generation

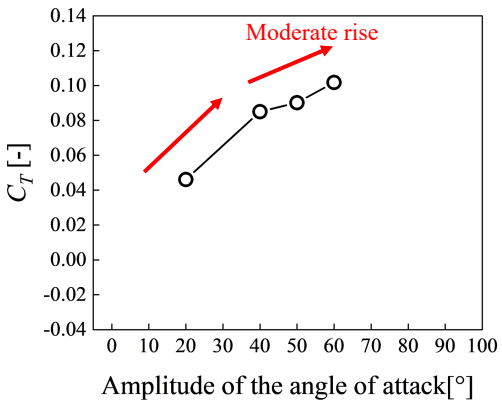

Thrust coefficient v AoA amplitude

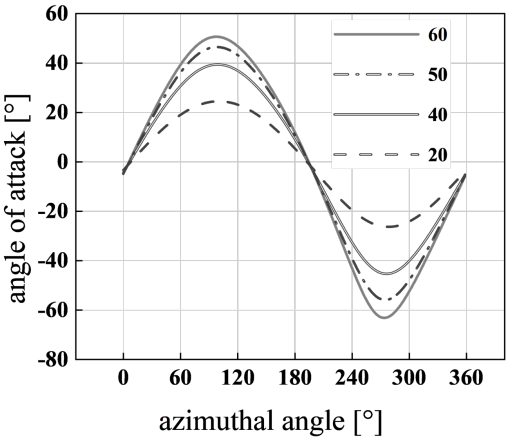

AoA schedules

12

Thrust generation: in detail

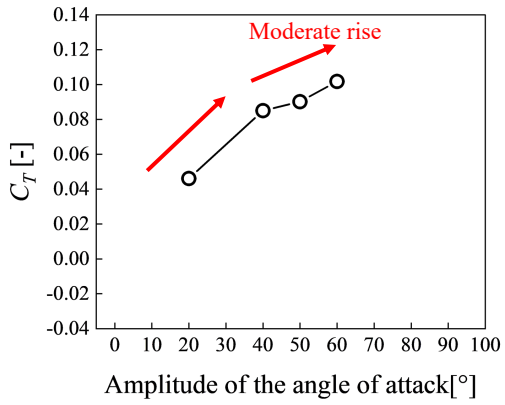

Thrust coefficient v AoA amplitude

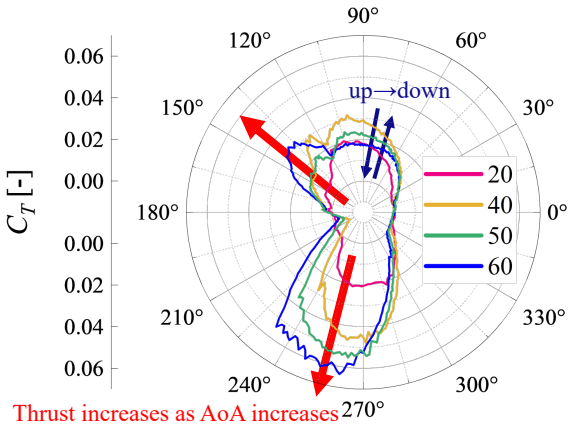

Azimuthal distribution of thrust coefficient

Sheldahl and Klimas, 1981. Sandia National Lab

13

Thrust generation: in detail

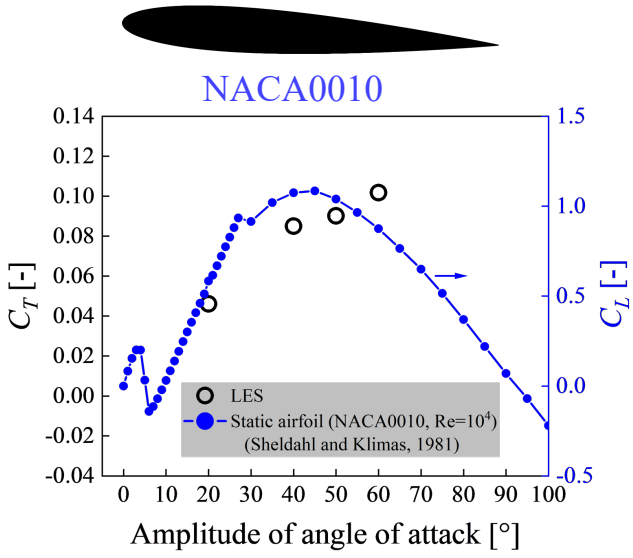

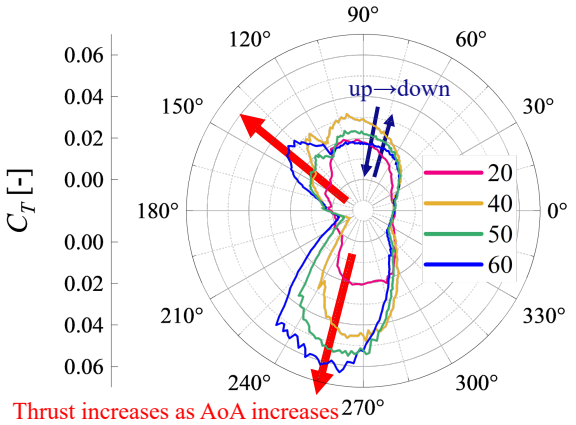

Azimuthal distribution of thrust coefficient

Sheldahl and Klimas, 1981. Sandia National Lab

14

Thrust generation: in detail

No more increase in thrust is expected
→ Max AoA: 40°

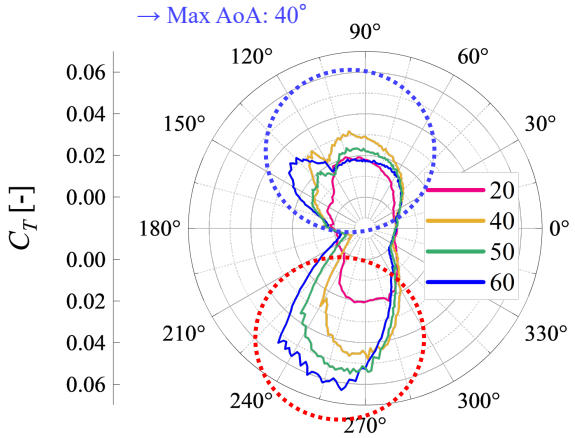

Increase in thrust is expected → Increase AoA

Azimuthal distribution of thrust coefficient

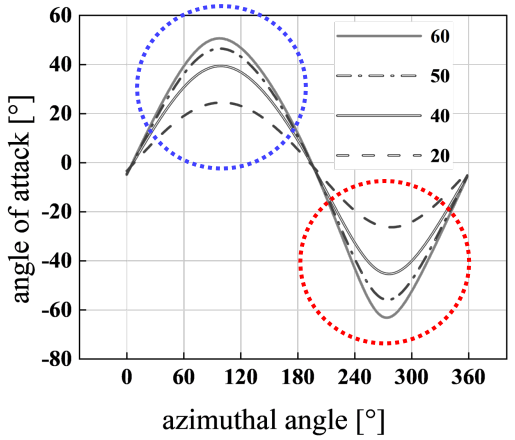

Current cyclorotors feature symmetrical AoA distribution in suction/blowing sides
→ Asymmetric design can be more efficient

ICCFD12

15

Proposing a new AoA schedule

No more increase in thrust is expected
→ Max AoA: 40°

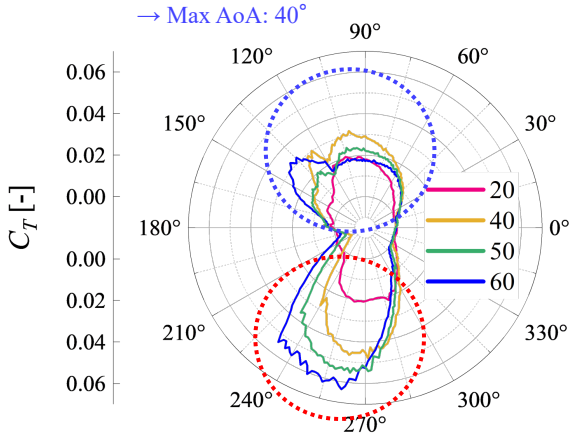

Increase in thrust is expected → Increase AoA

Azimuthal distribution of thrust coefficient

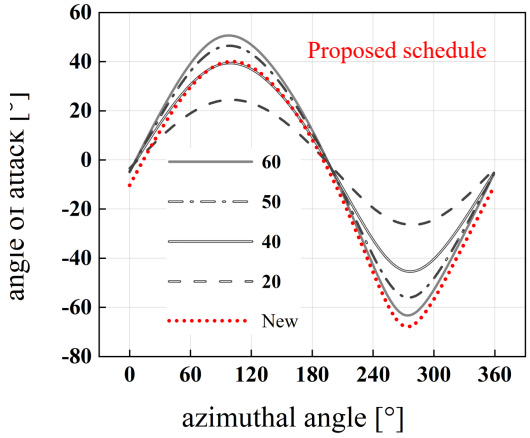

Current cyclorotors feature symmetrical AoA distribution in suction/blowing sides
→ Asymmetric design can be more efficient

ICCFD12

16

Thrust efficiency

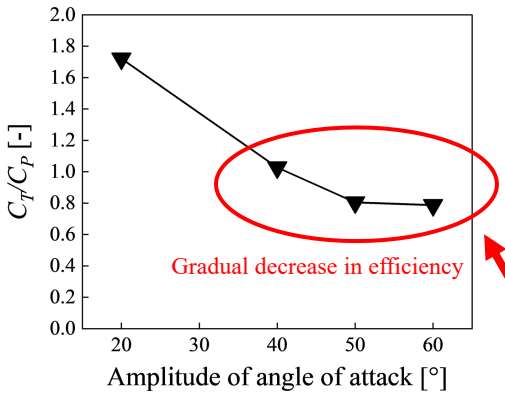

$$C_T = \frac{\text{Thrust}}{\rho \pi b_r d (\Omega R)^2}$$

$$C_P = \frac{\text{Power}}{\rho \pi b_r d (\Omega R)^3}$$

ρ : density
b_r : span length
d : Diameter
R : Radius
Ω : Rotational speed

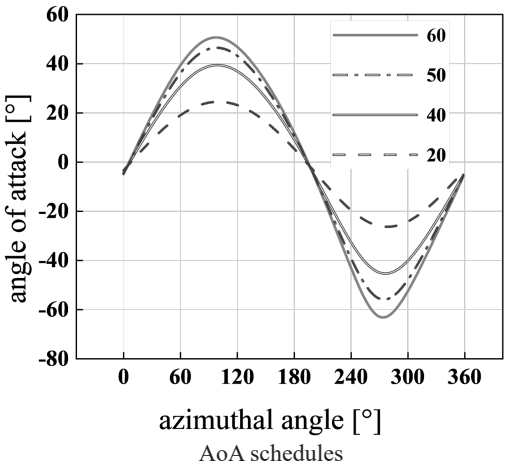

AoA schedules

Practical enough to apply large AoA amplitude (50°, 60°)

17

Conclusions

In this study, several LES of cyclorotors for different AoA amplitudes were performed to investigate the thrust generation characteristics of a cyclorotor. The main results can be summarized as follows:

1. Increasing the AoA amplitudes increases the thrust generation of a cyclorotor, but as the AoA amplitude becomes larger, the increase in thrust generation becomes moderate.
2. In the suction side of the cyclorotor, the increase in thrust generation peaks when the AoA amplitude is 40° and starts to decrease as the AoA amplitude becomes even larger.
3. In the blowing side of the cyclorotor, the thrust generation increases as the AoA amplitude increases up to the AoA amplitude of 60°.
4. Current cyclorotors feature symmetrical AoA distribution in the suction and the blowing sides, but to increase the thrust generation, the AoA distribution can be asymmetric: smaller AoA amplitude at the suction side (e.g., 40°); and larger AoA amplitude at the blowing side (e.g., 65°).

18